A METHOD FOR THE EARLY DETECTION OF INSTABILITIES IN ROTORDYNAMICS

Grant NAG8-119

For the period
27 December 1988 - 26 December 1989

Performed for
NASA Marshall Space Flight Center

Performed by
Department of Algebra, Combinatorics, and Analysis
Auburn University
Auburn University, AL 36849-5307

Principal Investigator: Richard A. Zalik

ABSTRACT

For a simple Jeffcott model with deadband, we develop a method to determine stability margins by an analysis of the Discrete Fourier transform of the system response. The viability of this method is demonstrated by means of numerical simulations. We also explain the circular behavior of the system response on the stability boundary.

INTRODUCTION

In this report we develop a method to determine stability margins for a simple Jeffcott model with deadband. We consider an unbalanced, uniform, flexible shaft supported by bearing, that rotates along the x axis. If m is the mass of the shaft, y and z describe the displacement of the center of the shaft, $r = (y^2 + z^2)^{1/2}, h(t) = 1$ if $r \leq \delta$ and $h(t) = \delta/r$ if $r > \delta$, then our model is represented by the following system of coupled nonlinear differential equations:

$$\begin{aligned} y'' + Cy' + [A + K(1 - h(t))]y + Bz &= f_1(t) \\ z'' + Cz' - By + [A + K(1 - h(t))]z &= f_2(t), \end{aligned} \tag{1}$$

where the coefficients have the following physical interpretation: $C = C_s/m, A = K_s/m, K = K_b/m, B = Q_s/m$ where C_s is the seal damping, K_s the seal stiffness, K_b the bearing stiffness, and Q_s denotes the cross-coupling stiffness of the seals. We assume that $f_1(t)$ and $f_2(t)$ are arbitrary continuous and bounded functions. In the particular case in which the shaft rotates with angular velocity w, and no sideloads or other factors are present, $f_1(t) = d_m w^2 \cos wt, f_2(t) = d_m w^2 \sin wt$, and d_m is the displacement of the shaft's center of mass from the geometric center. A sketch of our model can be seen in Fig. 1, with the caveat that the seals are not shown. To say that our model is stable, is the same as saying that all the solutions of the system of differential equations (1) are bounded.

THEORETICAL ANALYSIS

This is a review of results obtained in [1], to which the reader is referred for additional details. This paper was motivated by previous work of Day [2], Yamamoto [3], and Childs [4]. See also Rowan [5].

Setting $M = A + K - iB, \mu = y + iz, q = h\mu, f = f_1 + if_2$, multiplying the second equation in (1) by i and adding it to the first one, we see that (1) is equivalent to

$$\mu'' + C\mu' + M\mu - Kq = f(t). \tag{2}$$

In order to study the stability of (2) we first study the stability of the linearized system

$$\mu'' + C\mu' + M\mu = f(t). \tag{3}$$

It can be shown that the solutions μ_ℓ of (3) have the form

$$\mu_\ell = c_1 \exp(\lambda_1 t) + c_2 \exp(\lambda_2 t) + \mu_p, \tag{4}$$

where μ_p is a particular solution of (3), λ_1 and λ_2 are the roots of $\lambda^2 + C\lambda + M = 0$, and c_1, c_2 are arbitrary constants. It is also known that $\lambda_1 = \alpha + i\beta, \lambda_2 = \alpha' - i\beta$, where α, α' and β are real and $\alpha' < \alpha$. Clearly $\beta/2\pi$ is the natural frequency of the linear system (3). The following inequalities will be useful in the sequel:

$$\begin{aligned} &\text{If } \alpha < 0, \text{ then } \tfrac{B}{C} < \beta < \sqrt{A+K}, \text{ and } \alpha' < 0 \\ &\text{If } \alpha = 0, \text{ then } \tfrac{B}{C} = \beta = \sqrt{A+K}, \text{ and } \alpha' < 0 \\ &\text{If } \alpha > 0, \text{ then } \tfrac{B}{C} > \beta > \sqrt{A+K} \end{aligned} \tag{5}$$

We have shown in [1] that, if $G(t) = (\lambda_1 - \lambda_2)^{-1}[\exp(\lambda_1 t) - \exp(\lambda_2 t)]$, then every solution μ of (2) can be represented in the form $\mu(t) = \mu_\ell(t) + P(t)$, where

$$P(t) = K \int_0^t G(t-x) \cdot q(x) dx.$$

Since $|q(t)| \leq \delta$, it readily follows that $P(t)$ is bounded whenever $\alpha < 0$. An inspection of (4) readily shows that this is the same condition that guarantees the boundedness of μ_ℓ. In other words, (2) is stable if and only if the linearized system (3) is stable. However, since the coefficients of (2) are in general not very well known, this conclusion does not have a straightforward application. We shall now see that, nevertheless, it can be used in an analysis of the discrete Fourier transform of the system response $\mu(t)$.

Let $a_{k,n} = nd + k\xi, k = 0, \ldots, m-1, d = m\xi, m$ and ξ constant, and

$$D_n\mu(\lambda) = m^{-1} \sum_{k=0}^{m-1} \mu(a_{k,n}) \exp(-i\lambda a_{k,n}).$$

Assume $\mu(t) =$ transients $+\sum_{k=0}^{\infty} b_k e^{i\sigma_k t}$, with $\sum_{k=0}^{\infty} |b_k| < \infty$, and let $\lambda_j, j = 0, \ldots, N$ be given. Then, for any $\epsilon > 0$ there are ξ and m such that

$$D_n\mu(\lambda_j) = D_n\mu_p(\lambda_j) + K[(A + K - \lambda_j^2) + i(C\lambda_j - B)]^{-1} D_n q(\lambda_j) + E_{j,n},$$

and $|E_{j,n}| < \epsilon, j = 0, \ldots, N, n = 0, 1, 2, \ldots$ We have therefore obtained the approximate identity

$$D_n\mu(\lambda_j) \doteq D_n\mu_p(\lambda_j) + K[(A+K-\lambda_j^2)] + i(C\lambda_j - B)]^{-1} D_n q(\lambda_j), j = 0, \ldots, N \tag{6}$$

Note that we *have not* assumed that the signal is band limited. Most of the remainder of this report deals with material that will appear in [6].

APPLICATIONS

We define the (theoretical) *stability margin* SMT of the system represented by (2), by means of the identity

$$SMT = |(A + K - \beta^2) + i(C\beta - B)|/K$$

In view of (5), $SMT \to 0$ as $\alpha \to 0$. Thus, if $D_n\mu_p(\beta) \doteq 0$ (which would happen if for instance $f(t) = A_0 \exp(iwt)$ and $\beta \neq w$), we infer from (6) that SMT could be computed as the ratio of $|D_n q(\beta)|$ and $|D_n\mu(\beta)|$.

In practice, the value of β is of course unknown. However, if $D_n q(\beta)$ does not vanish as $\alpha \to 0$, the right hand member of (5), evaluated at $\lambda_j = \beta$, would diverge as $\alpha \to 0$. This would mean that the graph of $|D_n\mu(\lambda)|$ would exhibit a spike at some frequency $f_{n\ell}$ (which we shall call the *nonlinear* natural frequency) that approaches $\beta/2\pi$ as $\alpha \to 0$ (i.e. the linear and nonlinear natural frequencies coalesce) and that the magnitude of the spike would generally increase as α decreases. Thus, the ratio $|D_n q(\lambda)/D_n\mu(\lambda)|$ evaluated at $\lambda = 2\pi f_{n\ell}$ is an approximation to SMT and should yield an estimate of the stability margin of the system.

EXAMPLES

We consider (2) with initial conditions $\mu(0) = \delta, \mu'(0) = 0$, and $A = 0, C = 240, \delta = 0.0000285, K = 1,305,000, d_m = 0.000060915, w = 1,000\pi s, B = 60w$, where s varies. The linear natural frequency $\beta/2\pi$ will be denoted by f_0. The forcing frequency f_1 clearly equals $w/2\pi$, or 500s. The critical frequency f_c is the value of f_0 when $\alpha = 0$. From (4) we have $f_c = \sqrt{A+K}/(2\pi) = 181.8Hz$. Since $\frac{B}{C} = \sqrt{A+K}$, solving for s we readily deduce that this

frequency corresponds to $s_c = 1.4545$. This is the same example that we studied in [1].

In Table 1 we compare linear and nonlinear natural frequencies for various values of s, and different sampling intervals and sample sizes, and verify the assertion that both frequencies coalesce. We also observe that the location of the nonlinear frequency is practically independent of sampling interval and sample size.

In Table 2 we estimate stability margins, defined as the ratio $|D_n q / D_n \mu|$ computed at the location of the nonlinear natural frequency. We note that for each sampling interval and sample size the computed stability margins decrease as α increases. Tables 1 and 2 have been obtained from numerical solutions of the examples using a fourth order Runge-Kutta method followed by a Fast Fourier Transform algorithm. This procedure simulates an analysis of samples of the system response obtained through displacement probes. However, in many situations these probes are unavailable or yield inaccurate measurements and therefore accelerometer data becomes the only reliable kind available. To obtain the Discrete Fourier transform of μ from the Discrete Fourier transform of μ'', we can use the approximate identity

$$D_n \mu''(\lambda) \doteq -\lambda^2 D_n \mu \lambda), \tag{7}$$

which can be readily deduced from the mathematical analysis developed in [1].

In Fig. 2(a) we plot the absolute value of $D_n u$ for $s = 1.3$ and 1001 points in the interval $2.56 \leq t \leq 3.56$. The same plot, obtained from $D_n \mu''(\lambda)$ using (7), is shown in Fig. 2(b). Note that both plots are identical, except at low frequencies. Fig. 3 shows a plot of the absolute value of $D_n q$ (obtained by a simulation of a displacement probe), for the same range of parameters that was used in Fig. 2.

Formula (7) suggests a method to determine stability margins from accelerometers: Given a sample of the acceleration μ'' of the system response, compute $D_n \mu(\lambda_j), j = 0, \ldots, N$ using (7). To find $D_n q$, do an inverse Fourier transform to estimate $\mu(t)$. From μ it is then possible to estimate $q(t)$. For each value of t, this estimate will be very inaccurate. However, it is reasonable to expect that for sufficiently large N these errors will even out, yielding a reasonable good estimate of $D_n q$. The feasibility of this method

is demonstrated in Table 3.

ANNULAR VS. CIRCULAR BEHAVIOR

It was observed by Day [2] that near the stability boundary the system response has circular behavior, and there has been some intertest in finding an explanation for this phenomenon. The explanation is, in fact, very simple: Fig. 4 shows a plot of $|D_n\mu|$ on the stability boundary. Clearly the nonlinear natural frequency f_0 dominates all other frequencies, and therefore $D_n\mu(\lambda) \doteq A_0\delta(\lambda - f_0)$, where δ denotes Dirac's delta function. Inverting, we have $D_n\mu(\lambda) \doteq A_1 \exp(if_0t)$. Fig. 5 exhibits the circular behavior of the system response on the stability boundary.

MAJOR POINTS

* Proof that nonlinear frequency approaches the frequency of instability at the stability boundary

* PSD of displacement can be obtained from PSD of acceleration

** Given knowledge of the location of the nonlinear spike and of the psd of acceleration, a real time direct calculation of stability margin can be made

* An explanation of circular solutions vs. annular

* Methods have been proven only on a simple, low order system

* Physical proof of the method on a real system is the next logical step

REFERENCES

1. R. A. Zalik, The Jeffcott equations in nonlinear rotordynamics, Quarterly of Applied Mathematics 47 (December 1989), 585-599.

2. W. B. Day, Asymptotic expansions in nonlinear rotordynamics, Quarterly of Applied Mathematics 44 (1987), 779-792.

3. T. T. Yamamoto, On critical speeds of a shaft, Mem. Fac. Engineering, Nagoya Univ. 6 (1954), 106-174.

4. D. W. Childs, The space shuttle main engine high-pressure fuel turbopump rotordynamics instability problem, Trans. ASME, J. Engineering for Power, 48-57 (January 1978).

5. B. F. Rowan, Rotordynamics Technical Manual, Rockwell International, Rocketdyne Division, Canoga Park, California, November 1981.

6. R. A. Zalik, Determination of stability margins for a simple Jeffcott model, to appear in "Proceedings of the International Congress on recent developments in air and structure borne sound and vibration", Auburn University, March 1989.

TABLES AND FIGURES

s	alpha	f0	d=1	d=128
1.3	-12.63	181.61	163	162.74
1.35	-8.54	181.68	169	168.78
1.4	-4.45	181.74	175	175.00
1.45	-0.37	181.81	181	181.25
1.4545	-4.51E-4	181.81	181	181.80
1.5	3.71	181.88	182	181.51

Table 1. Comparison of Linear and nonlinear natural frequencies. Column three shows linear natural frequencies. Columns four and five show observed nonlinear natural frequencies for intervals of the form $(2.56, 2.56 + d)$. The results in column four were obtained using both 2^{11} and 2^{18} points. The values obtained were the same. For column five, 2^{18} points were used.

s	alpha	SMT	$n = 2^{11}$ d=1	$n = 2^{18}$ d=1	$n = 2^{18}$ d=128
1.3	-12.63	2.22E-2	1.99E-1	1.99E-1	1.99E-1
1.35	-8.54	1.50E-2	1.38E-1	1.38E-1	1.38E-1
1.4	-4.45	7.83E-3	7.35E-2	7.35E-2	7.36E-2
1.45	-0.37	6.47E-4	8.71E-3	8.71E-3	6.18E-3
1.4545	-4.51E-4	7.93E-7	5.01E-3	4.99E-3	1.75E-4
1.5	3.71	6.54E-3	2.06E-7	2.06E-7	2.07E-212
1.6	11.85	2.09E-2	2.48E-19	2.49E-19	

Table 2. Determination of stability margins. The third column lists the theoretical stability margins. Columns four, five and six list stability margins computed from intervals of the form $[2.56, 2.56 + d]$, with sample size n, sample rate $1/n$, and d and n as indicated.

s	α	SMT	$d = 1$ $n = 2^{12}$	$d = 1$ $n = 2^{18}$	$d = 128$ $n = 2^{18}$
1.3	-12.63	2.22E-2	4.84E-3	1.92E-3	2.03E-1
1.35	-8.54	1.50E-2	2.05E-3	8.92E-4	5.21E-2
1.4	-4.45	7.83E-3	3.80E-2	1.59E-2	6.78E-2
1.45	-0.37	6.47E-4	4.57E-4	4.15E-4	5.08E-3
1.4545	-4.51E-4	7.93E-7	4.25E-5	1.17E-5	2.82E-5

Table 3. Determination of stability margins from simulated accelerometer data. Columns four, five and six list stability margins computed from intervals of the form [2.56, 2.56 $+d$], with sample size n, sample rate $1/n$, and d and n as indicated.

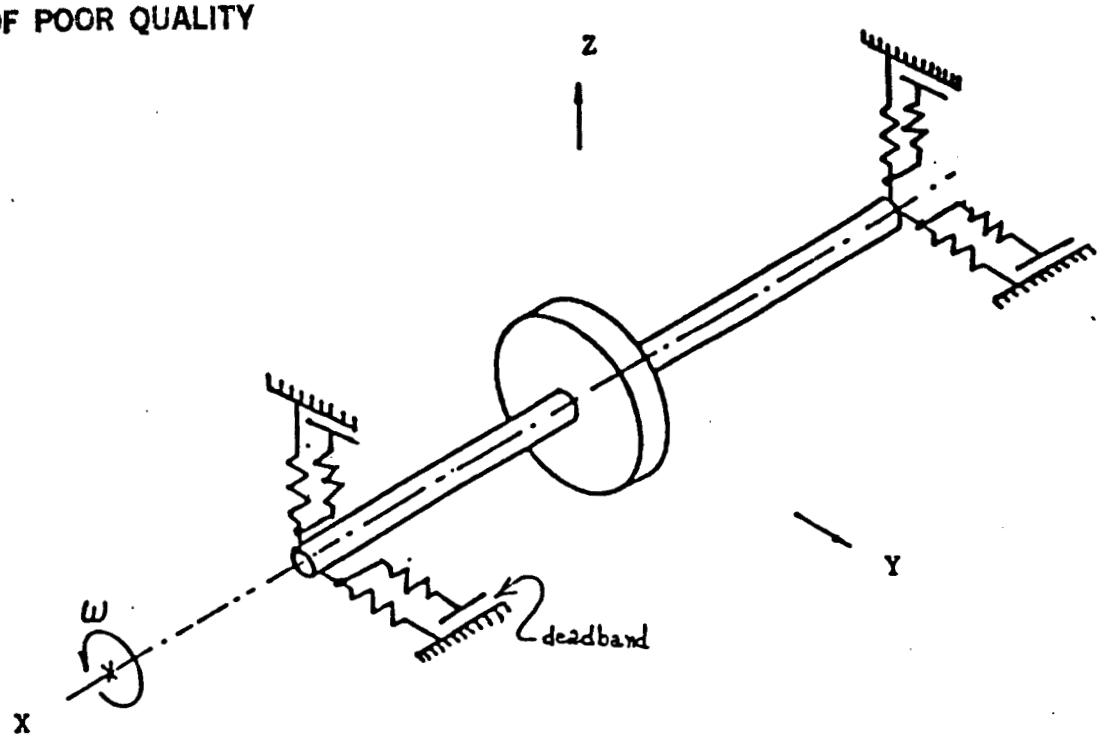

FIG. 1

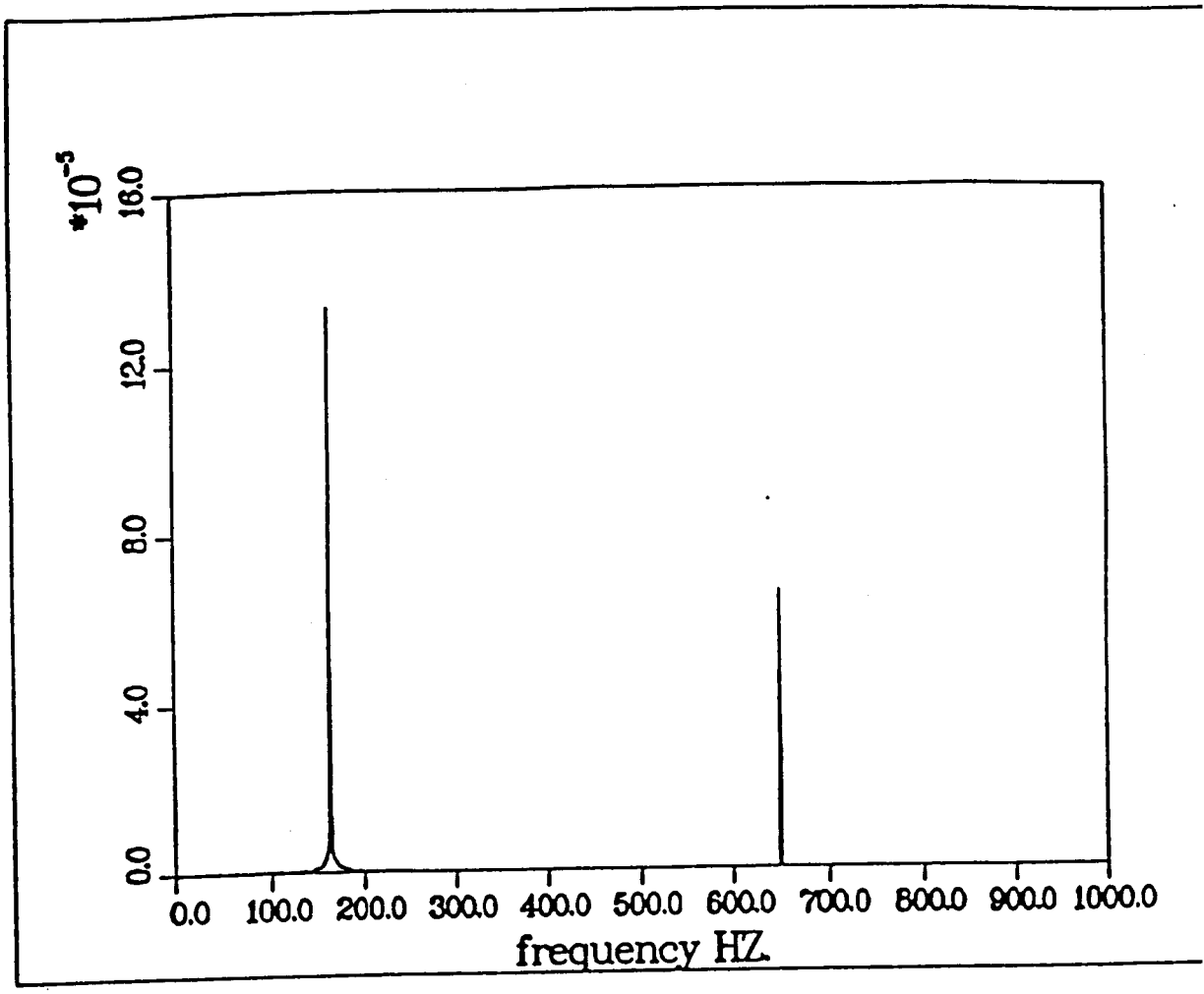

$$s = 1.3, 2.56 < t < 3.56, 1001 pts.$$

Fig. 2(a)

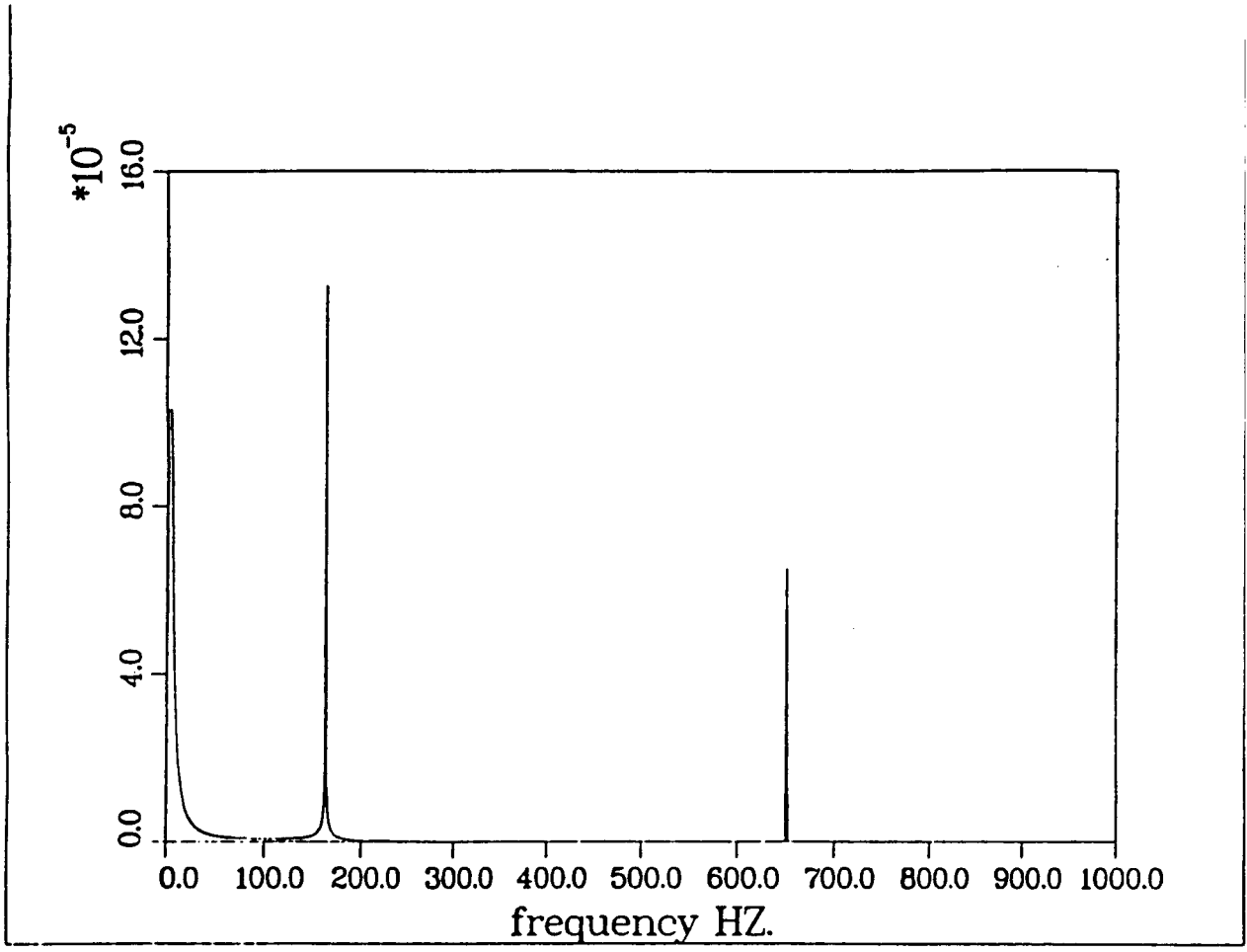

s = 1.3, 2.56 < t < 3.56
PSD plot of μ obtained from PSD plot of μ''

Fig. 2(b)

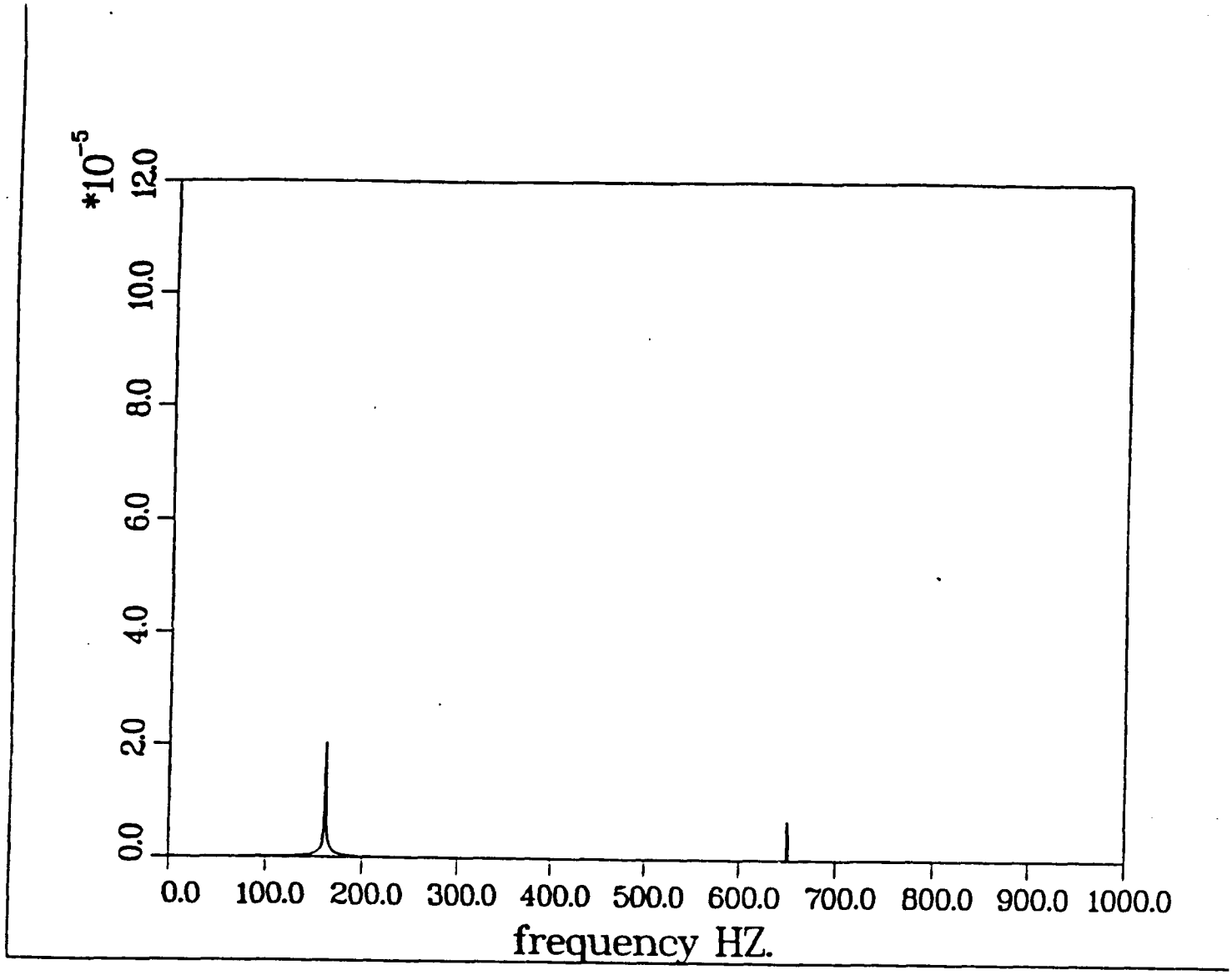

PSD plot for q, s = 1.3
2,56 < t < 3.56, 1001 points

Fig. 3

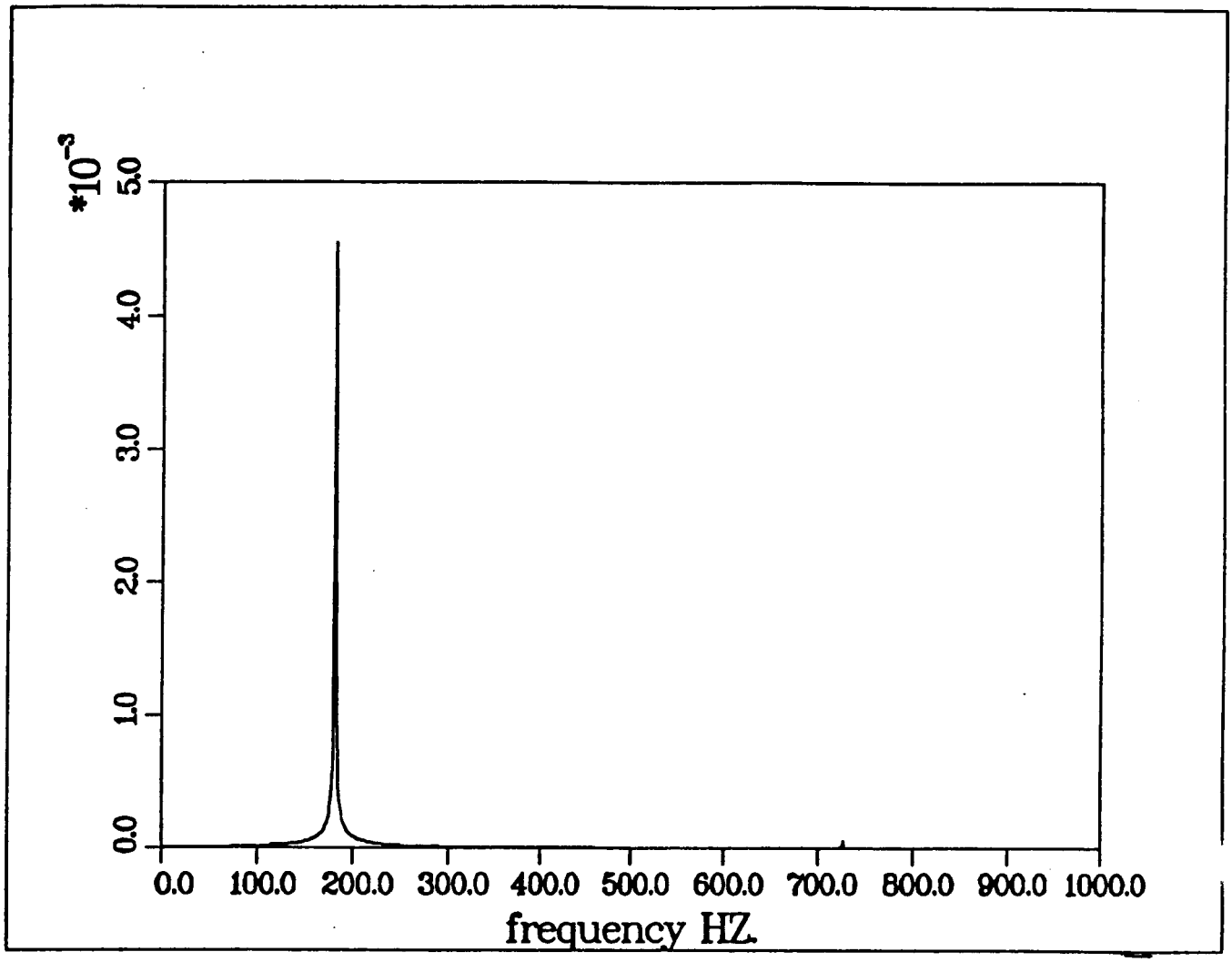

PSD plot for s = 1.454505522, 2.56 < t < 3.56

value at f_0: $4.55*10^{-3}$

value at f_1: $5.9*10^{-5}$

Fig. 4

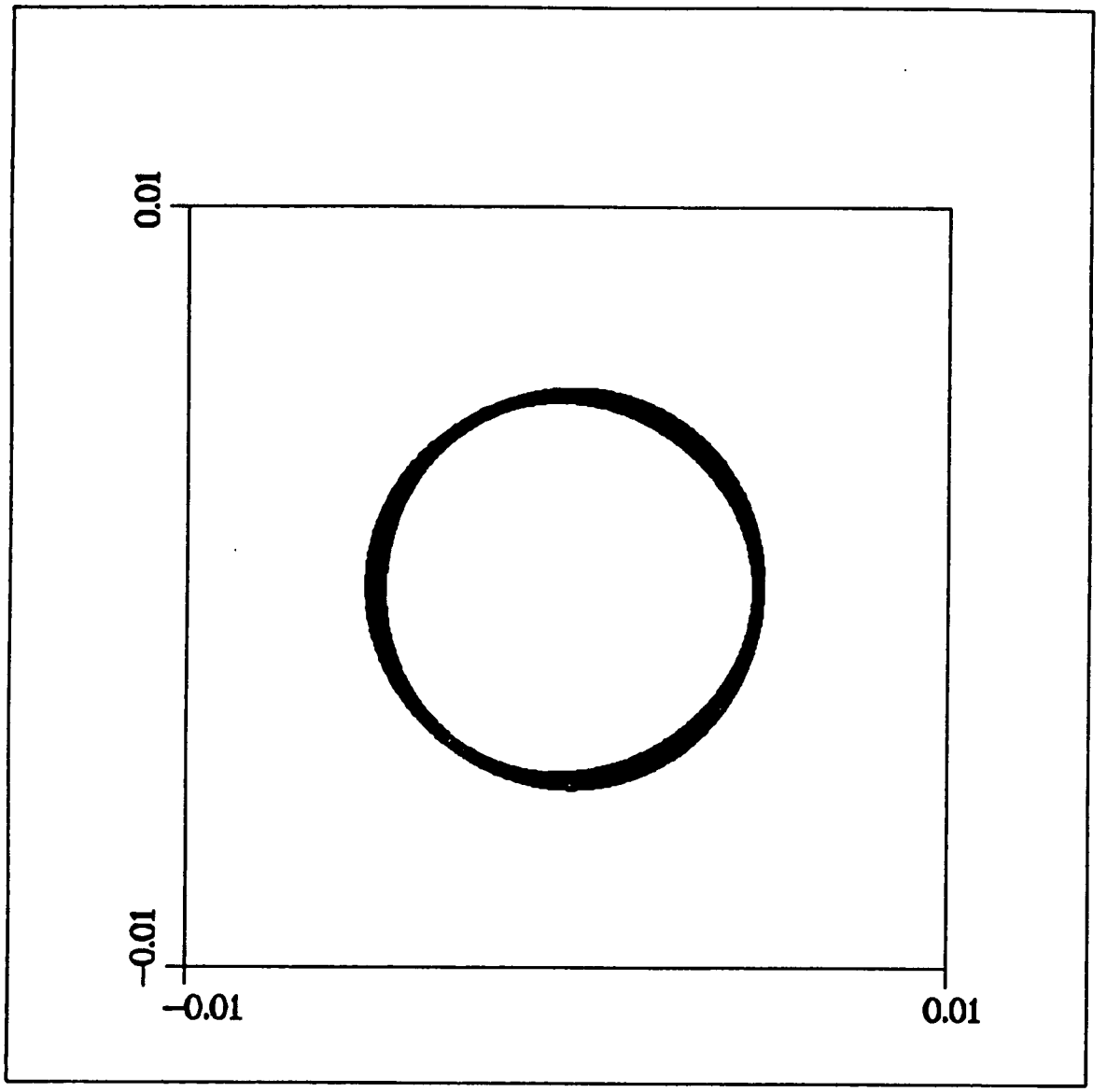

$2.56 < t < 2.81$, 2^{15} points,

$s = 1.454505522$, $\alpha = -2{,}59*10^{-8}$

$\min|\mu(t)| = 4.78*10^{-3}$, $\max|\mu(t)| = 5.33*10^{-3}$

Fig. 5